RESEARCH ARTICLE

# Plasma surface modification and three-dimensional structuring of additively manufactured polyetheretherketone implants for improvement of osseointegration

**Lea Strauss[1]** 🔘  |  **Arnaud Bruyas[2]**  |  **Raul Gonzalez[3]**  |  **Daphne Pappas[3]**  |
**Dhia Ben Salem[4]** 🔘  |  **Erhard Krampe[4]**  |  **Thomas Schmitt-John[4]**  |
**Stefan Leonhardt[2]**

[1]Department of Mechanical Engineering, University of the Bundeswehr Munich, Neubiberg, Germany

[2]Kumovis GmbH, Munich, Germany

[3]Plasmatreat USA, Hayward, California, USA

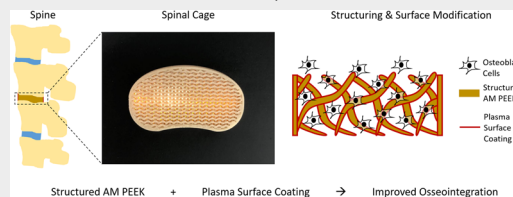[4]Plasmatreat GmbH, Steinhagen, Germany

**Correspondence**
Lea Strauss, Chair of Materials Engineering, Department of Mechanical Engineering, University of the Bundeswehr Munich, 85577 Neubiberg, Germany.
Email: lea.strauss@unibw.de

## Abstract

Osseointegration is highly desirable for implants used for bone replacement. Polyetheretherketone (PEEK) is an attractive material due to its characteristics such as high biocompatibility and Young's modulus similar to human bones. However, PEEK is bioinert, meaning cells do not adhere and proliferate on its surface. This problem is addressed in this study, with the goal of enhancing osseointegration of additively manufactured PEEK. The influences of surface modifications and porous structures on cellular behavior were assessed by wettability and in vitro tests with subclone of the human osteosarcoma cell line-2 osteoblasts. Overall, the combination of surface modification, type of plasma process used, atmospheric pressure versus vacuum-based, and surface structuring, especially gyroid structures, improve the cellular proliferation on PEEK. Therefore, its ability to enhance osseointegration is highly promising.

## 1  |  INTRODUCTION

The successful integration of implants with surrounding bone tissue, known as osseointegration, is vital for establishing a stable anchorage and a functional bone–implant interface through direct bone-to-implant contact.[1] If this prerequisite is not fulfilled, undesirable effects, like inflammatory or allergic reactions as well as fibrous encapsulations, can take place. For the patient, such effects can lead to implant dislodging and rejection, which can be resolved by surgical replacement.[2,3] As reported by Gristina et al.,[4] three properties of a bone implant are identified as important selection criteria for successful osseointegration: the material, the surface, and the design.

With respect to the mechanical properties, the material should present a high resistance to external forces like

bending, compression, and traction, while simultaneously having Young's modulus similar to the surrounding bone tissue (cortical bone: 13.8 GPa, spongy bone: 1.38 GPa[5]).[3,6] Nowadays, titanium is one of the most implanted materials because of its bioinertness, high fatigue strength, nontoxicity,[7] and osseointegration ability.[8] However, the high Young's modulus of titanium (110 GPa) leads to "stress shielding,"[9] an inhomogeneous stress transfer between the implant and the surrounding bone, which can lead to implant loosening.[10] The usage of titanium as bone implant material is thus debated. Besides this, titanium also generates artifacts in screening methods like computed tomography (CT) and magnetic resonance imaging (MRI).[9] High-performance polymers like polyetheretherketone (PEEK) can overcome these challenges.[7] PEEK is well known in medical technology for its biocompatibility, its compatibility with screening techniques like MRI and CT, as well as its Young's modulus (3-4 GPa[11]) similar to that of human bones.[12] Furthermore, a study in the clinical and radiological field comparing titanium and PEEK spinal cages has shown a better outcome with PEEK.[13] The authors showed that PEEK led to significantly fewer complications (PEEK: 36.6%, titanium: 64%) and fewer surgical replacements (PEEK: 2.97%, titanium: 16%). PEEK is already used as an alternative to titanium for spinal surgeries, fracture fixation, joint replacement, and maxillofacial operations.[14–16] However, one disadvantage of PEEK is its bioinert character[17] leading to limited cell proliferation on its surface. The poor osseointegrative performance prohibits the widespread utilization of PEEK in surgical fracture treatment.

Adequate physical and chemical characteristics of the implant surface are essential for a successful osseointegration.[18,19] For example, it has been shown that wettability has a strong influence on cellular behavior, and that cells exhibit improved adhesion and proliferation on hydrophilic surfaces.[20,21] The relative hydrophobicity of unmodified PEEK can therefore partially explain its bioinert character[22] and can be overcome through the application of surface modification (SM) methods. Numerous SM techniques have already been explored, such as the deposition of coatings, surface functionalization through the grafting of new chemical groups, and surface patterning.[20,23] In addition to SM, surface topography has a strong influence on cell proliferation. In this regard, an optimal surface would mimic biological tissues and therefore present a porous design with bioinspired macrostructures.[3] The porosity strongly influences cell proliferation. Indeed, higher porosity leads to a higher surface area, whereby more surface is available for protein binding, and therefore an enhanced connection to the surrounding tissue is possible.[20] The size of the pores also influences the transportation of cells, nutrients, and growth factors through blood flow.[24] Recently, additive manufacturing (AM) has been proven able to manufacture such macrostructures.[25,26] As an added advantage, the freedom in design inherent to this technology can be utilized to produce new cell-friendly three-dimensional (3D) structures[25] and patient-specific implants, which improves osseointegration due to optimal design.[27]

The aim of the study presented in this article was to evaluate the impact of different SMs and macrostructures on the cellular behavior, the adhesion and proliferation properties, of PEEK produced through an AM method, and study the factors leading to successful osseointegration. First, the impact of plasma-based surface treatments on wettability as well as on cytotoxicity according to DIN EN ISO 10993 was studied. In the second step, the effects of the SMs on cell proliferation were evaluated. In addition to this, the influence of surface structuring, developed through the AM process, on cellular proliferation was analyzed. Finally, we tested the influence of the combination of both SMs and structuring on cell proliferation. Such a combination was studied, to the extent of our knowledge, for the first time.

## 2 | MATERIALS AND METHODS

### 2.1 | Parts manufacturing

The different samples for cellular testing were designed and converted into standard tesselation language data, containing information about the surface geometry of 3D objects, using SolidWorks (Dassault Systèmes SolidWorks Corp.). For the eluate cytotoxicity tests, parallelepipeds with the dimensions 50 mm × 10 mm × 1 mm were fabricated. The parts for the two-dimensional (2D) cell proliferation were additively manufactured wells: each cylinder was 15.7 mm in diameter and had a height of 7 mm, with a bottom and a wall thickness of 2 mm. The 3D proliferation tests were performed on parts presenting different macrostructures. In the design process, a solid cylinder with a diameter of 13 mm and a height of 5 mm was sliced via Simplify3d or Slic3r to create macrostructures (n = 3 samples for each macrostructure and modification). The macrostructures of samples A, B, and C are shown in Figure 3a. For structure A, a rectilinear fill pattern resulting in a surface area of 22.63 cm² was selected. For structures B and C, a gyroid fill pattern with a surface area of 16.05 and 17.52 cm² was chosen. For these 3D structures, the surface area was determined using micro-computed tomography (μCT) exaCT XS scanner

(Wenzel Volumetrik GmbH) and SolidWorks. For evaluating the pore size, measurements with SolidWorks, based on the μCT data, were performed.

Slicing was achieved with the software Simplify3D (Simplify3D, Inc.) and Slic3r (Version 1.3.0, www.slic3r.org). Test specimens were prepared with an AM prototype provided by Kumovis GmbH (Munich) based on the technology of Fused Layer Manufacturing (FLM). The samples were manufactured with commercially available polyetheretherketone KetaSpire® MS NT1 (Solvay S. A.), using a filament diameter of 1.75 mm. The main printing parameters are shown in Table 1.

## 2.2 | Surface modifications

Four distinct SM processes, labeled as SM1–SM4, were selected to enhance the surface characteristics of additively manufactured PEEK parts. Untreated PEEK specimens served as control (SM0). Table 2 summarizes the SM parameters and depicts the various types of SM that were employed.
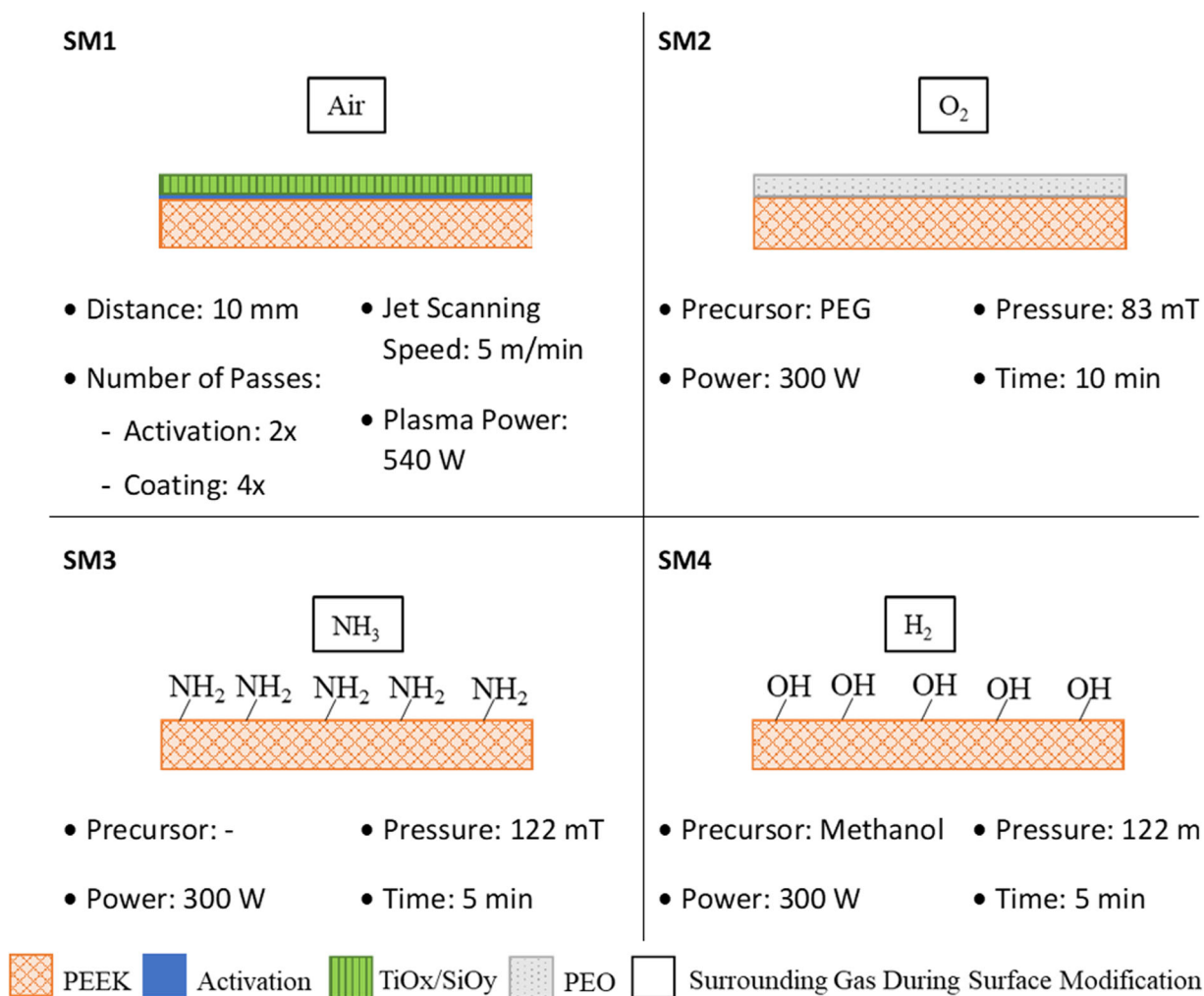
For SM1, the open-air plasma technology PlasmaPlus® (Plasmatreat GmbH) was used. A TiOx/SiOy precursor was introduced directly in the plasma. Samples were activated twice with a plasma jet scanning speed of 5 m/min and at a

**TABLE 1** Printing parameters for all manufactured PEEK test specimens.

| Nozzle diameter | Printing speed | Extrusion width | Layer thickness | Extruder temp. | Chamber temp. | Bed temp. |
|---|---|---|---|---|---|---|
| 0.4 mm | 1200 mm/min | 0.3 mm | 0.2 mm | 400°C | 260°C | 250°C |

Abbreviation: PEEK, polyetheretherketone.

**TABLE 2** Representation and parameters of surface modification processes.



**SM1**

Air

- Distance: 10 mm
- Number of Passes:
  - Activation: 2x
  - Coating: 4x
- Jet Scanning Speed: 5 m/min
- Plasma Power: 540 W

**SM2**

O₂

- Precursor: PEG
- Power: 300 W
- Pressure: 83 mT
- Time: 10 min

**SM3**

NH₃

NH₂ NH₂ NH₂ NH₂ NH₂

- Precursor: -
- Power: 300 W
- Pressure: 122 mT
- Time: 5 min

**SM4**

H₂

OH OH OH OH OH

- Precursor: Methanol
- Power: 300 W
- Pressure: 122 m
- Time: 5 min

PEEK    Activation    TiOx/SiOy    PEO    Surrounding Gas During Surface Modification

*Note*: For SM1, the technology PlasmaPlus®, and for SM2—SM4, Aurora Plus Low-Pressure Plasma System were used.

Abbreviation: SM, surface modification.

10 mm distance. The plasma power was 540 W, and the air was chosen as an ionization gas. For the coating process, the plasma jet nozzle was moved four times over the parts under the parameters described above. For the other three processes (SM2–SM4), the low-pressure plasma system Aurora Plus system (Plasmatreat USA Inc.), a plasma-enhanced chemical vapor deposition (PECVD) platform, was used for the functionalization (Processes SM3 and SM4) and deposition of nanocoatings (Process SM2) using low-pressure (vacuum) plasma. More specifically, process SM2 resulted in the deposition of polyethylene oxide (PEO)-like coatings, while samples exposed to SM3 and SM4 were functionalized through the grafting of amine groups and hydroxyl groups. For SM2, a PEO coating was created by derivating the diethylene glycol dimethyl ether precursor (diglyme, Fisher Scientific). The liquid precursor was vaporized in an evaporator at a temperature of 70°C and the vapor was carried to the plasma chamber with a carrier gas. For SM3, an amine functionalization of PEEK was performed by exposing the substrates to an NH3 plasma. Here, positively charged –NH2 functional groups were expected to be grafted on the surface due to plasma treatment. For SM4, the functionalization of PEEK with hydroxyl groups was performed in a methanol-based plasma. At this, OH groups were grafted at the surfaces.

## 2.3 | Wettability

The ability of an implant to transport liquid and nutrition can be estimated indirectly by determining its wettability. The contact angle was determined using the sessile drop method according to DIN EN 828. Drop Shape Analyzer DSA25E (Krüss GmbH) and the related software Advance 1.8. (Krüss GmbH) were used to perform the analysis. A total of 2 µL droplets of distilled water were placed at a speed of 2 µl/s on the test surfaces ($n = 10$ droplets on each sample). The dimension of the samples was 50 mm × 10 mm × 1 mm.

## 2.4 | Cell culture

Mammalian osteoblasts of cell line subclone of the human osteosarcoma cell line-2 (SAOS-2) (DSMZ, Braunschweig) were used for evaluating in vitro cytotoxicity of the different PEEK modifications, as well as in vitro cell proliferation on 2D and 3D manufactured and modified PEEK structures. Cells were cultured in Mc Coy's 5 A modified medium (w 2.2 g/l NaHCO3), supplemented with 10.9% fetal bovine serum (FBS) (Thermo Fisher Scientific), 2.44% NaHCO3, 1.12% L-Glutamine, 1% Penicillin-Streptomycin (Sigma-Aldrich), and 1% Amphotericin B (Sigma-Aldrich), and incubated at 37°C and 10% $CO_2$-atmosphere.

## 2.5 | Eluate cytotoxicity tests

Eluate testing was performed according to the standard DIN EN ISO 10993. For each eluate, three parallelepipeds were incubated in the cell culture medium (see Section 2.4) for 72 h at 37°C and 10% CO2-atmosphere. Cells were seeded in five wells of a 96-multiwell plate at a density of 5000 cells/cm² ($i = 5$ of 96 multititer wells) for the eluate testing. Subsequently, the seeded cells were incubated in the cell culture medium for 24 h. After the completion of the 24 h incubation process, cells were inoculated with the eluates and incubated for a further 72 h. Afterward, a cell counting kit-8 assay was performed by measuring mitochondrial cell activity via the water-soluble tetrazolium-8 (WST-8) assay (Dojindo Molecular Technologies Inc.). According to the manufacturer's instructions, a WST-8–cell culture medium solution (ratio 1:11) was put on the cells and incubated for 1 h. To evaluate the proliferation rate, the solution was read in a Multiskan FC Microplate Photometer (Thermo Fisher Scientific Inc.) at 450 and 620 nm. Cell culture medium and control copper eluate were used as negative (=100%) and positive controls, respectively.

## 2.6 | 2D proliferation tests

For the 2D proliferation tests, SAOS-2 osteoblasts were seeded with a density of 5000 cells/cm² on the bottom of the additively manufactured well ($n = 3$ for each SM), where the cells were allowed to grow. After 7 days of incubation at 37°C and 10% $CO_2$-atmosphere, the WST-8 assay (Dojindo Molecular Technologies Inc.) was performed according to the manufacturer's instructions. The WST-8–cell culture medium solution (ratio 1:11) was put on the cells and incubated for 1 h. To evaluate the proliferation rate, the solution was put in additional multititer wells ($n = 4$ wells) and read in the Multiskan FC Microplate Photometer (Thermo Fisher Scientific Inc.) at 450 and 620 nm. As control groups, 96-well multititer wells with cell repellent coatings (Greiner Bio One International GmbH) as well as multititer wells generally used in cell culture were, respectively, defined as negative and positive (=100%) controls. Using the measured adsorption values, the proliferation rates were evaluated relative to the confluent positive control and normalized by each seeded cell density.

## 2.7 | 3D proliferation tests

To evaluate the cell proliferation, samples were first deposited in multititer wells filled with cell culture medium. Afterward, cells were seeded with a density of 1768, 872, and 913 osteoblasts/cm² for structures A, B, and C, respectively.

For all, the structures were incubated for 7, 14, and 21 days at 37°C and 10% $CO_2$-atmosphere. Every 7 days and immediately before the proliferation tests, the structures were moved into a new well with fresh cell culture medium to quantify only adherent cells. Cell proliferation was evaluated by using the tetrazolium salt WST-8. According to the manufacturer's instructions, a WST-8–cell culture medium solution (ratio 1:11) was put on the cells and incubated for 1 h. Multititer wells with cell-repellent coatings were defined as negative control. As a positive control, cells were seeded in a generally used multititer well to be confluent after 7 days. For both control groups, a density of 5000 osteoblasts/cm² was used. Using the measured adsorption values, the proliferation rates were evaluated relative to the confluent positive control (=100%) after 7 days of incubation and normalized by the seeded cell density.

Furthermore, phase contrast microscopy of the multititer wells with removed macrostructures was used to qualitatively evaluate the effectiveness of the 3D structures and SMs concerning the influence on cellular adhesion and proliferation.

## 2.8 | Statistical analysis

For all evaluations, a minimum number of three samples was used. Statistical analysis was performed using Origin 2019 (OriginLab, Corp.). Statistical significance was identified using an independent two-sample $t$ test, and for the 3D proliferation tests, one-way analysis of variance (ANOVA) with Tukey's multiple comparison method was

used. For all tests, a $p$-value $< 0.05$ (*, □ resp. Δ) was considered as significant. The results of the experiments were represented using box plots. For the box plots, the median (central line), the first and third quartile (box), and the upper and lower whiskers are illustrated.

# 3 | RESULTS

## 3.1 | Wettability

The results of the contact angle measurements showed an average value of 90° for SM0, an indication that the surface of the 3D-printed PEEK samples without any treatment was hydrophobic (Figure 1a). All SMs significantly lowered the contact angle. The average contact angles were 49° ± 12°, 56° ± 4°, 64° ± 8°, and 55° ± 4° for SM1, SM2, SM3, and SM4, respectively.

## 3.2 | Eluate cytotoxicity tests

Results of cytotoxicity tests are detailed in Figure 1b, including the control copper eluate. All tested samples presented a proliferation higher than 70%, the limit value for cytotoxic behavior according to DIN EN ISO 10993. However, all modified surfaces showed significantly lower proliferations than the one on untreated PEEK with values of 91%, 91%, 87%, and 96%, respectively, for SM1, SM2, SM3, and SM4. For SM1, some flakes were observed with phase microscopy.
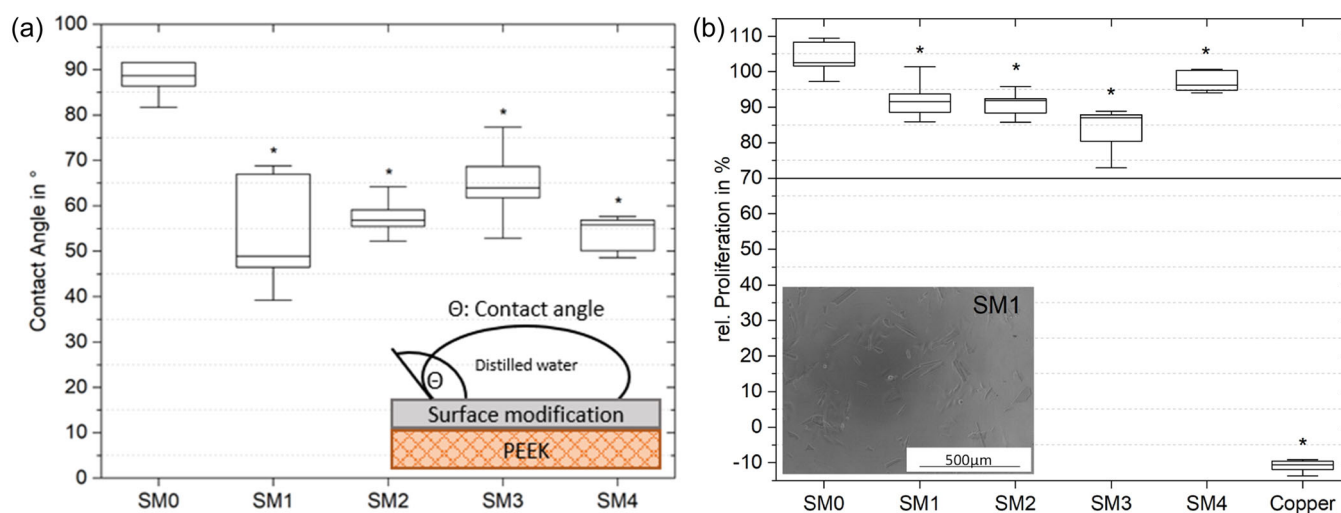


**FIGURE 1** Surface modification. (a) Contact angle measurements on the treated surfaces. (b) SAOS-2 cell proliferation on the treated and untreated surfaces, the copper control eluate, and a microscopic image of the SM1 eluate with flakes. For cytotoxicity, the proliferation was determined relative to confluent cells inoculated with cell culture medium (negative control = 100%). A relative proliferation smaller than 70% indicates a cytotoxic behavior. *represents statistical significance ($p < 0.05$). SAOS-2, subclone of the human osteosarcoma cell line-2.

## 3.3 | 2D proliferation test

In the 2D proliferation tests, cell proliferation rates after 7 days of incubation were higher on modified surfaces than on untreated ones (see Figure 2). On untreated SM0 control samples, proliferation rates of 12% were measured. SM1 showed the highest proliferation values with 28%, whi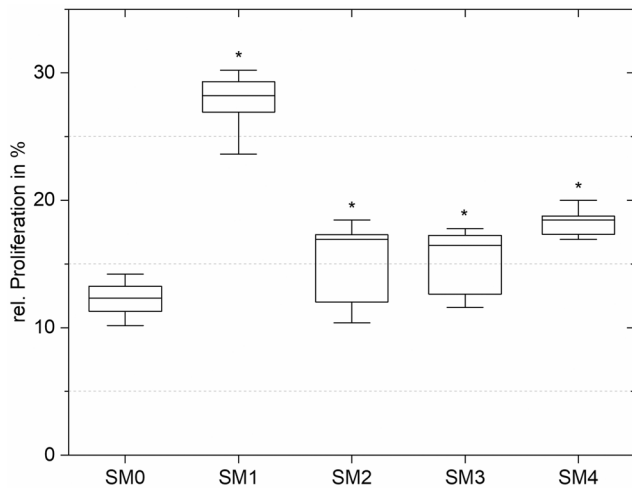le SM2 and SM3 samples had similar proliferation rates of about 16%, and SM4 showed 18%. All SMs caused a significant increase in proliferation rates compared with SM0 controls.

## 3.4 | 3D proliferation tests on structured PEEK

The porous structures with various infill patterns and therefore different available surface areas for the cell attachment and proliferation (see Figure 3a) were investigated: rectilinear (structure A) and gyroid (structures B and C). For the gyroid structures, different pore sizes were evaluated.

In Figure 3b, the results of the 3D cell proliferation tests as well as the influence of PEEK surface macrostructures on cellular behavior are illustrated. All structures showed an improvement in cell proliferation dependent on the incubation time—the longer the incubation, the higher the proliferation. The highest cellular proliferation was observed for structure C at Day 7, 14, and 21, with a value of 76% reached at day 21.

## 3.5 | 3D proliferation tests on structured and modified PEEK

Figure 4 illustrates the impact of the combination of previously evaluated SMs (SM1–SM4) with the different 3D structures (A, B, and C) on cellular proliferation.



**FIGURE 2** Relative proliferation of two-dimensional (2D) surface polyetheretherketone (PEEK) parts. Proliferation rates were determined relative to confluent cells grown in a generally used multititer well after 7 days of incubation (positive control = 100%). Compared with SM0, stars (*) are considered to represent statistical significance ($p < 0.05$).
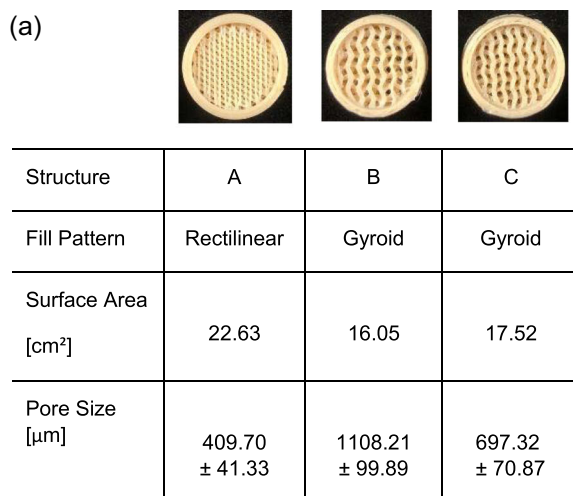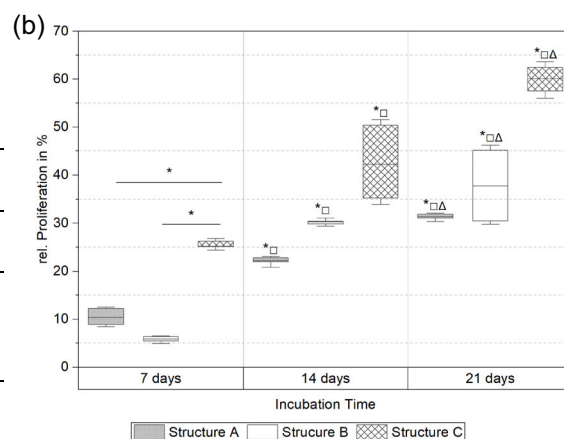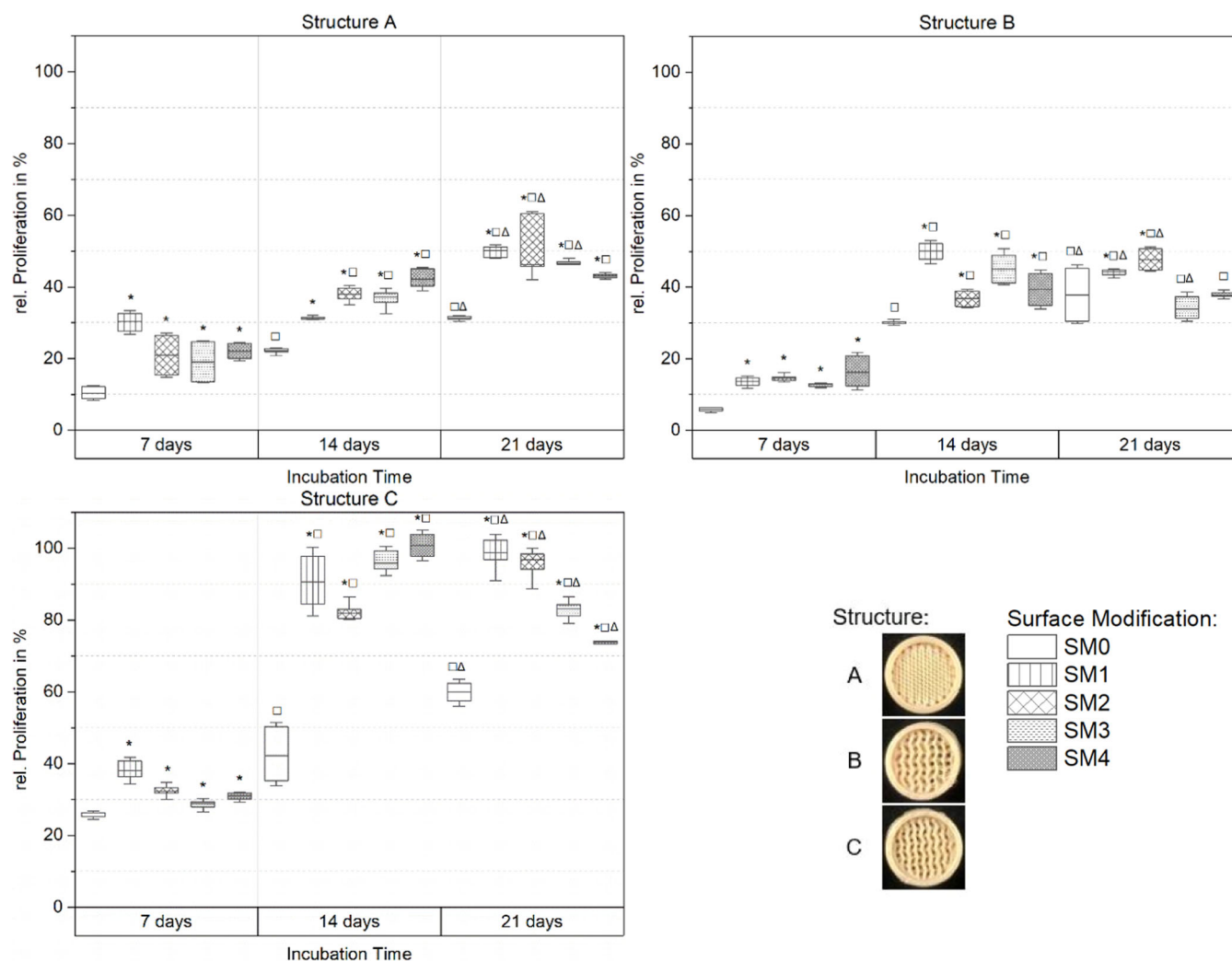


| Structure | A | B | C |
|---|---|---|---|
| Fill Pattern | Rectilinear | Gyroid | Gyroid |
| Surface Area [cm²] | 22.63 | 16.05 | 17.52 |
| Pore Size [µm] | 409.70 ± 41.33 | 1108.21 ± 99.89 | 697.32 ± 70.87 |



**FIGURE 3** Three-dimensional (3D) surface structures. In (a), different surface structures of polyetheretherketone (PEEK) are shown. The evaluated structures were 0°/60°/120°/−60°/−120° with a pore size of 409.70 ± 41.33 µm (a) and gyroid with pore sizes of 1108.21 ± 99.89 µm (b) as well as 697.32 ± 70.87 µm (c), determined using µCT. In (b), the results of the three-dimensional (3D) cell proliferation tests on untreated PEEK structures a, b, and c are illustrated. For the cellular tests, the proliferation rates were determined relative to confluent cells grown in a generally used multititer well after 7 days of incubation (positive control = 100%) and normalized by each seeded cell density. * is considered as statistical significance ($p < 0.05$) between the surface modifications for each time point. □ represents statistical significance between the proliferation rates for each modification at different time points: between Day 7 and 14, as well as Day 7 and 21 of incubation. Comparing the proliferation rates of each modification after Day 14 and 21, statistical significance is marked with Δ. µCT, micro-computed tomography.

**FIGURE 4** Cell proliferation on the modified three-dimensional (3D) polyetheretherketone (PEEK) structures A, B, and C. Here, the proliferation rates were determined relative to confluent cells grown in a generally used multititer well after 7 days of incubation (positive control = 100%) and normalized by each seeded cell density. Compared with SM0, * is considered as statistical significance ($p < 0.05$) for each time point. □ represents statistical significance between the proliferation rates for each modification at different time points: between Day 7 and 14, as well as Day 7 and 21 of incubation. Comparing the proliferation rates of each modification after Day 14 and 21, statistical significance is marked with Δ.

Compared with the 2D proliferation tests on flat modified PEEK samples, structure C is the only 3D structure that increased proliferation rates for each evaluated SM. Here, structure C led to the highest determined proliferation rates for each of the modifications.

For all structures, except structure B at day 21, the modifications improved cell proliferation compared with untreated PEEK. With increasing the incubation time, an improvement in proliferation rates is observed. For structure A, cell proliferation reached average values of 50% for the modified samples. Test specimens of structure B presented for all surfaces after 21 days with approximately 40% cell proliferation. Even after 14 days of incubation, structure C had proliferation rates around 100% for most SMs. The highest evaluated proliferation rates were found for structure C and SM4 after 14 days of incubation.

Phase contrast microscopy showed for all SMs for structure B a large quantity of adherent cells at the bottom of the multititer wells. Compared with that, a lower quantity was found for structure A and even less for structure C. In the cell culture medium supernatants of SM1 samples, some flakes were detected.

# 4 | DISCUSSION

PEEK is an attractive material for bone replacement due to its advantages such as biocompatibility, compatibility with screening techniques, and similar mechanical properties to

that of human bones under tensile compressive loads. Nonetheless, its bioinert character restricts its usage as bone implant material. In this study, we explored the improvement of bioinert, additively manufactured PEEK due to various SMs and structures as well as the combination of both.

## 4.1 | Wettability

SM0, with a contact angle near 90°, is assumed not to be optimal for osseointegration due to its low wettability. Compared with SM0, all evaluated SMs improved the wettability of PEEK. SM1 showed, beside SM4, the highest wettability.

The improvement of SM1 is caused by TiOx, which forms stable hydroxyl groups that lead to an attractive interaction with water molecules, resulting in a super hydrophilic surface.[28,29] Mixing with hydrophobic SiOy results in a contact angle between those of super hydrophilic TiOx and hydrophobic SiOy.[30] The high standard deviation might be due to coating instability. Spalling is seen in the cell culture medium, caused by either weak binding of the coating to the PEEK surface or degradation of the coating itself during incubation in the cell culture medium.

The hydrophilic character of SM2 is caused by the formation of polyethylene oxide (PEO)-like thin films resulting from the plasma polymerization of diglyme.[26,31]

The enhanced wettability of SM3 samples is assumed to be attributed to the positively charged amino groups that mediate the hydrophilic properties of the surface. The SM4 modification of PEEK leads to hydroxyl groups on the surface. As evaluated by Marchand-Brynaert et al.,[32] this kind of surface is more attractive for water, as compared with TiO.

The positive effect of PEG surfaces as well as the surface functionalization with amino- and hydroxyl groups was reported by Noiset et al.,[15] where PEEK was modified with the same substrate but through selective wet chemistry. In their study, functionalization with amino groups led to a moderate wettability, while PEG and hydroxyl groups showed a hydrophilic character with even better wettability.

Overall, these results indicate that wettability can be largely improved via SMs, which is expected to enhance cellular proliferation. A hydrophilic implant leads to better wetting in physiological fluids. The hydrophilic character of the modified surfaces tends to resist the adsorption of proteins, followed by cell attachment on the surfaces.[20]

## 4.2 | Eluate cytotoxicity tests

According to DIN EN ISO 10993, a reduction of cell proliferation below 70% compared with the blank sample is classified as cytotoxic. Thus, none of the SMs showed cytotoxic effects. However, the observed flaking of the SM1 coating in the eluate is not desirable since this could lead to fibrous encapsulation in vivo.

## 4.3 | 2D proliferation tests

Compared with SM0, all modifications led to significantly better cell proliferation on flat surfaces after 7 days of incubation. Similar results were demonstrated by Rapp et al. and Buxadera-Palomero et al.[30,33] Besides wettability, properties like surface chemistry, Young's modulus, topography, and surface roughness might cause enhanced cell proliferation.[20,34] The positive effect of TiOx/SiOy coatings, like SM1, on cell proliferation was also demonstrated by Rapp et al.[30] The mixture of TiOx and SiOy is generally known as hydrophilic, mechanically stable, biocompatible, and antimicrobial. Furthermore, silicon oxide layers are known to support cell growth.[18,35]

An influence similar to that of SM2 was observed in studies of Buxadera-Palomero et al.[33] They detected a correlation between wettability and protein adsorption on PEO coatings and demonstrated that the adsorption of the cell adhesion-inhibiting protein albumin was lowered on the PEG. This phenomenon might explain the improved cell attachment on SM2. Pan et al.[36] furthermore showed that plasma-deposited tetraethylene glycol dimethyl ether provides a PEG-like coating exhibiting nonfouling properties, stability in aqueous environments, resistance to ethanol sterilization, and reduced nonspecific protein adsorption. In addition, the good coating stability detected by Kane et al.[37] showed the suitability of PEG-coatings for cell attachment in tissue engineering due to their hydrophilic nature, which reduces nonspecific protein adsorption, facilitates lubrication, and enhances cell spreading and attachment on various surfaces.

The effects of SM3- and SM4-like coatings were also evaluated by Lee et al. and Bozzini et al.[38,39] An enhanced cell proliferation by functionalized surfaces with amine- and hydroxyl groups on different basic materials was demonstrated, supposedly due to the hydrophilic character of the surfaces.[38] It is assumed that SM3 and SM4 coatings lead to a positive surface charge of the samples, and since most cell and protein surfaces are negatively charged, an electrostatic interaction promoting cell adhesion on the sample surfaces can be expected.[40,41] Boespflug et al. also detected the positive influence of N-rich surfaces on both cell adhesion and growth.[42]

Our assumption, that the enhancement of cellular proliferation is due to improved wettability, was supported by the results of the 2D cell proliferation tests,

where all tested SMs caused improved proliferation rates compared with unmodified SM0.

## 4.4 | 3D proliferation tests on structured PEEK

As seen in the results of the 3D cellular testing on SM0 (Figure 3b), structuring and porosity had a high influence on cell proliferation. The literature points out that 3D structures, that is, parts with high porosities, improve cellular in-growth.[3,43,44] This was also seen in our study by comparing the 3D cellular evaluations with the 2D surface proliferation tests after 7 days of incubation in wells with various structures and pore sizes. When comparing to 2D surface proliferation tests, the influence of the pore size and porous structure[20,45] is evident. Structure C is the only surface topology that showed significantly higher cellular proliferation rates than the other samples.

After 7, 14, and 21 days of incubation, our results suggest that gyroid structure C is the most promising of the evaluated macrostructures for osseointegration. Zaharin et al.[46] also demonstrated promising results of porous scaffolds, using gyroid structures with characteristics similar to natural bone, and Spece et al. reported a positive influence of gyroid structures on cellular ingrowth as well.[25,47] The pore size of their PEEK structures ($669 \pm 216\,\mu m$[47] as well as $708 \pm 64\,\mu m$[25]) caused an obvious improvement in cell proliferation after 7 and 14 days of incubation, compared with unstructured PEEK parts.

As seen qualitatively by microscopic inspection, most adherent cells were detected at the bottom of the wells with structure A. Based on De Wild et al., who showed in their studies[34,48] that a pore size above $500\,\mu m$ had a positive influence on cellular behavior, we expect that the rectilinear structure (structure A) is not as good as gyroid for supporting proliferation and thereby osseointegration. Similar studies of Spece et al.[25,47] demonstrated a significant influence of gyroid surface topology. Furthermore, pore size appears to influence cellular adhesion, whereby structure C with a smaller pore size (structure B: $1108.21 \pm 99.89\,\mu m$, structure C: $697.32 \pm 70.87\,\mu m$) showed fewer adherent cells on the bottom of the well. This is in line with Spece et al., who also detected promising proliferation rates with comparable pore sizes.[25]

## 4.5 | 3D proliferation tests on structured and modified PEEK

As seen in the 2D in vitro evaluation, the 3D proliferation tests showed even after 7 days of incubation that all modifications tested improved cellular proliferation, compared with the unmodified SM0. As already mentioned in the 2D proliferation tests, this could be caused by the enhanced capillary effect as a consequence of SM.

The synergistic effect of the structures in combination with SMs caused better results than structuring and modification separately. The structuring, in combination with the chemical SM, opens up promising possibilities for improved osseointegration. Of all the different types of modification, structure C showed the highest proliferation rates, illustrating the importance of SM of bioinert materials as well as the pore size and the type of porous structure.[20] After 14 days of incubation, nearly the whole modified structure is covered with SAOS-2 osteoblasts for all SMs. However, the highest proliferation rates (100.7%) were found on SM1 and SM4 after 14 days of incubation.

The flaking of SM1, detected in cytotoxicity assays, might be attributed to the low adhesive strength of the coating due to a less ideal layer thickness or occurrence of voids. Thus, SM1 coating is to be improved to enhance stability and homogeneity and to prevent complications like inflammation, allergic reactions, or fibrous encapsulations.

Overall, the highest cellular proliferation was achieved with the combination of structure C and SM4 coating after 14 days of incubation.

Wettability plays an important role in osseointegration,[20,21] and this was clearly supported by our results of the 2D and 3D cell proliferation tests. All surfaces with increased hydrophilic properties showed improved cell proliferation compared with the rather hydrophobic untreated PEEK samples.

## 5 | CONCLUSIONS

In our study, the surfaces of additively manufactured PEEK parts were modified with plasma-enhanced coatings as well as porous structuring, and for the very first time, the combination of both methods for 3D-printed PEEK samples was evaluated. For SM, TiOx/SiOy and PEG/PEO coatings as well as functionalization with amino- and hydroxyl groups were investigated. No SM showed cytotoxic effects on SOAS-2 osteoblasts according to the standard DIN EN ISO 10993 cytotoxicity tests. We demonstrated improved cellular activity on a modified 2D PEEK surface compared with pure PEEK. 3D structures of PEEK surfaces were tested, documenting the influence of design and pore size. Gyroid structures appear to have better effects on cell growth and viability compared with rectilinear structures for osseointegration. A gyroid pore size of approx. $697.32\,\mu m$ showed

after 7 days of incubation a higher cell viability as on flat 2D PEEK samples. After 14 days of incubation, the entire surface of the structured PEEK samples was covered with SAOS-2 osteoblast cells. In addition, the combination of SM and porous structures showed further enhancement of cell growth and osseointegration. PEEK with gyroid surface structure with a pore size of $697.32 \pm 70.87\,\mu m$ and combined with hydroxyl group functionalization showed the best results. In general, our results demonstrated a strong correlation between wettability and cell proliferation. All tested SMs showed improved contact angles and caused increased cell proliferation, and thus will lead to improved osseointegration of modified PEEK implants.

## AUTHOR CONTRIBUTIONS

The manuscript was written through the contributions of all authors. All authors have given approval to the final version of the manuscript.

## ACKNOWLEDGMENTS

## CONFLICT OF INTEREST STATEMENT

The authors declare no conflict of interest.

## DATA AVAILABILITY STATEMENT

The data that support the findings of this study are available from the corresponding author upon reasonable request.

## ORCID

*Lea Strauss* http://orcid.org/0000-0001-6541-8019
*Dhia Ben Salem* http://orcid.org/0000-0002-0340-2799

## REFERENCES

[1] T. Albrektsson, C. Johansson, *Eur. Spine J.* **2001**, *10 Suppl 2*, 96. https://doi.org/10.1007/s005860100282

[2] E. Wintermantel, S.-W. Ha (eds.) *Medizintechnik: Life Science Engineering*, Springer Berlin Heidelberg, Berlin, Heidelberg **2009**.

[3] R. Kramme, *Medizintechnik*, Springer Berlin Heidelberg, Berlin, Heidelberg **2017**.

[4] A. G. Gristina, P. Naylor, Q. Myrvik, *Med. Prog. Technol.* **1989**, *14*, 205.

[5] J. Knaus, D. Schaffarczyk, H. Cölfen, *Macromol. Biosci.* **2020**, *20*, 1900239. https://doi.org/10.1002/mabi.201900239

[6] E. Wintermantel, B. Shah-Derler, A. Bruinink, M. Petitmermet, J. Blum, S.-W. Ha *Medizintechnik: Life Science Engineering* (Eds: E. Wintermantel, S.-W. Ha), Springer Berlin Heidelberg, Berlin, Heidelberg **2009**, p. 67.

[7] S. G. Steinemann, *Periodontology 2000* **1998**, *17*, 7. https://doi.org/10.1111/j.1600-0757.1998.tb00119.x

[8] T. Albrektsson, P. I. Brånemark, H. A. Hansson, J. Lindström, *Acta Orthop. Scand.* **1981**, *52*, 155. https://doi.org/10.3109/17453678108991776

[9] A. E. Castellvi, A. Castellvi, D. H. Clabeaux, *J. Clin. Neurosci.* **2012**, *19*, 517. https://doi.org/10.1016/j.jocn.2011.06.029

[10] M. Niinomi, M. Nakai, *Int. J. Biomater.* **2011**, *2011*, 1. https://doi.org/10.1155/2011/836587

[11] L. Qin, S. Yao, J. Zhao, C. Zhou, T. W. Oates, M. D. Weir, J. Wu, H. H. K. Xu, *Materials* **2021**, *14*(2), 408. https://doi.org/10.3390/ma14020408

[12] L. M. Wenz, K. Merritt, S. A. Brown, A. Moet, A. D. Steffee, *J. Biomed. Mater. Res.* **1990**, *24*, 207. https://doi.org/10.1002/jbm.820240207

[13] C. Schulz, U. M. Mauer, R. Mathieu, *Z. Orthop. Unfall.* **2017**, *155*, 201. https://doi.org/10.1055/s-0042-118717

[14] P. Scolozzi, *Aesthetic Plast. Surg.* **2012**, *36*, 660. https://doi.org/10.1007/s00266-011-9853-2

[15] O. Noiset, Y. J. Schneider, J. Marchand-Brynaert, *J. Biomater. Sci., Polym. Ed.* **2000**, *11*, 767. https://doi.org/10.1163/156856200744002

[16] E. T. Camarini, J. K. Tomeh, R. R. Dias, E. J. Da Silva, *J. Craniofac. Surg.* **2011**, *22*, 2205. https://doi.org/10.1097/SCS.0b013e3182326f2c

[17] S. M. Kurtz, J. N. Devine, *Biomaterials* **2007**, *28*, 4845. https://doi.org/10.1016/j.biomaterials.2007.07.013

[18] S. Nilawar, M. Uddin, K. Chatterjee, *Mater. Adv.* **2021**, *2*, 7820. https://doi.org/10.1039/D1MA00733E

[19] J. r Novaes AB, S. L. de Souza, R. R. de Barros, K. K. Pereira, G. Iezzi, A. Piattelli, *Braz. Dent. J.* **2010**, *21*, 471. https://doi.org/10.1590/s0103-64402010000600001

[20] A. Nouri, C. Wen, in *Surface Coating and Modification of Metallic Biomaterials* (Ed: C. Wen), Woodhead Publishing, **2015**, p. 3. https://doi.org/10.1016/B978-1-78242-303-4.00001-6

[21] P. Gehrke, R. Jansen, G. Dhom, J. Neugebauer, *Z Zahnärztl. Impl.* **2006**, *22*, 29.

[22] P. Johansson, R. Jimbo, P. Kjellin, F. Currie, B. R. Chrcanovic, A. Wennerberg, *Int. J. Nanomed.* **2014**, *9*, 3903. https://doi.org/10.2147/IJN.S60387

[23] H. Zhang, Z. Guo, Q. Chen, X. Wang, Z. Wang, Z. Liu, *Thin Solid Films* **2016**, *615*, 63. https://doi.org/10.1016/j.tsf.2016.06.042

[24] X. Wang, S. Xu, S. Zhou, W. Xu, M. Leary, P. Choong, M. Qian, M. Brandt, Y. M. Xie, *Biomaterials* **2016**, *83*, 127. https://doi.org/10.1016/j.biomaterials.2016.01.012

[25] H. Spece, T. Yu, A. W. Law, M. Marcolongo, S. M. Kurtz, *J. Mech. Behav. Biomed. Mater.* **2020**, *109*, 103850. https://doi.org/10.1016/j.jmbbm.2020.103850

[26] A. Gebhardt, *Anwendungen. In 3D-Drucken*, Carl Hanser Verlag GmbH & Co. KG Munich, Germanyg, **2014**.

[27] A. Koptyug, L.-E. Rännar, M. Bäckström, M. S. S. Fager Franzén, D. P. Dérand, *Int. J. Life Sci. Med. Res.* **2013**, *3*, 15. https://doi.org/10.5963/LSMR0301003

[28] M. Vormoor, *Untersuchungen zur Superhydrophilie von Titandioxid-Beschichtungen*, Universität Hannover Cuvillier, Göttingen, Germany, **2009**.

[29] M. Amft, L. E. Walle, D. Ragazzon, A. Borg, P. Uvdal, N. V. Skorodumova, A. Sandell, *J. Phys. Chem. C* **2013**, *117*, 17078. https://doi.org/10.1021/jp405208x

[30] C. Rapp, A. Baumgärtel, L. Artmann, M. Eblenkamp, S. S. Asad, *Curr. Dir. Biomed. Eng.* **2016**, *2*, 43. https://doi.org/10.1515/cdbme-2016-0013

[31] C. H. Ho: Kern-Schale-Nanocontainer für funktionelle Metallnanopartikel und Wirkstoffe auf der Basis von hyperverzweigtem Polylysin. (Dissertation, Albert-Ludwigs-Universität Freiburg i. Br. **2009**).

[32] J. Marchand-Brynaert, G. Pantano, O. Noiset, *Polymer* **1997**, *38*, 1387. https://doi.org/10.1016/S0032-3861(96)00661-1

[33] J. Buxadera-Palomero, C. Calvo, S. Torrent-Camarero, F. J. Gil, C. Mas-Moruno, C. Canal, D. Rodríguez, *Colloids Surf., B* **2017**, *152*, 367. https://doi.org/10.1016/j.colsurfb.2017.01.042

[34] M. de Wild, R. Schumacher, K. Mayer, E. Schkommodau, D. Thoma, M. Bredell, A. Kruse Gujer, K. W. Grätz, F. E. Weber, *Tissue. Eng. Part. A.* **2013**, *19*, 2645. https://doi.org/10.1089/ten.TEA.2012.0753

[35] G. R. Beck, S. W. Ha, C. E. Camalier, M. Yamaguchi, Y. Li, J. K. Lee, M. N. Weitzmann, *Nanomed. Nanotechnol. Biol. Med.* **2012**, *8*, 793. https://doi.org/10.1016/j.nano.2011.11.003

[36] Y. V. Pan, T. C. McDevitt, T. K. Kim, D. Leach-Scampavia, P. S. Stayton, D. D. Denton, B. D. Ratner, *Plasmas Polym.* **2002**, *7*, 171. https://doi.org/10.1023/A:1016295419941

[37] S. R. Kane, P. D. Ashby, L. A. Pruitt, *J. Mater. Sci. Mater. Med.* **2010**, *21*, 1037. https://doi.org/10.1007/s10856-009-3935-6

[38] J. H. Lee, H. W. Jung, I. K. Kang, H. B. Lee, *Biomaterials* **1994**, *15*, 705. https://doi.org/10.1016/0142-9612(94)90169-4

[39] S. Bozzini, P. Petrini, M. C. Tanzi, C. R. Arciola, S. Tosatti, L. Visai, *Int. J. Artif. Organs* **2011**, *34*, 898. https://doi.org/10.5301/ijao.5000047

[40] J. H. Lee, J. W. Park, H. B. Lee, *Biomaterials* **1991**, *12*, 443. https://doi.org/10.1016/0142-9612(91)90140-6

[41] A. S. Curtis, J. V. Forrester, C. McInnes, F. Lawrie, *J. Cell. Biol.* **1983**, *97*, 1500. https://doi.org/10.1083/jcb.97.5.1500

[42] G. Boespflug, M. Maire, G. De Crescenzo, S. Lerouge, M. R. Wertheimer, *Plasma Processes Polym.* **2017**, *14*, 1600139. https://doi.org/10.1002/ppap.201600139

[43] R. G. Flemming, C. J. Murphy, G. A. Abrams, S. L. Goodman, P. F. Nealey, *Biomaterials* **1999**, *20*, 573. https://doi.org/10.1016/s0142-9612(98)00209-9

[44] H. Effenberger, M. Imhof, U. Witzel, S. Rehart, *Der Orthopäde*, *34*, 477.

[45] F. Liu, Z. Mao, P. Zhang, D. Z. Zhang, J. Jiang, Z. Ma, *Mater. Des.* **2018**, *160*, 849. https://doi.org/10.1016/j.matdes.2018.09.053

[46] H. Zaharin, A. Abdul Rani, F. Azam, T. Ginta, N. Sallih, A. Ahmad, N. Yunus, T. Zulkifli, *Materials* **2018**, *11*, 2402. https://doi.org/10.3390/ma11122402

[47] H. Spece, T. Yu, A. W. Law, M. M. S. Kurtz (ed.). In vitro response to FFF printed porous PEEK surfaces. 4th International PEEK Meeting, Washington, 2019.

[48] M. Wild, de S. Zimmermann, J. Rüegg, R. Schumacher, T. Fleischmann, C. Ghayor, F. E. Weber, *3D Print. Addit. Manuf.* **2016**, *3*, 142. https://doi.org/10.1089/3dp.2016.0004